Proc. Natl. Acad. Sci. USA
Vol. 93, pp. 2640–2645, April 1996
Biophysics

Potentiation of proton transfer function by electrostatic interactions in photosynthetic reaction centers from *Rhodobacter sphaeroides*: First results from site-directed mutation of the H subunit

(bacterial reaction center/proton transfer/electron transfer/quinone/site-directed mutagenesis)

EIJI TAKAHASHI AND COLIN A. WRAIGHT

Department of Plant Biology and Center for Biophysics and Computational Biology, University of Illinois, 1201 West Gregory Drive, Urbana, IL 61801

Communicated by Charles J. Arntzen, Boyce Thompson Institute for Plant Research, Inc., Ithaca, NY, October 30, 1995

ABSTRACT **The x-ray crystallographic structure of the photosynthetic reaction center (RC) has proven critical in understanding biological electron transfer processes. By contrast, understanding of intraprotein proton transfer is easily lost in the immense richness of the details. In the RC of *Rhodobacter (Rb.) sphaeroides*, the secondary quinone (Q_B) is surrounded by amino acid residues of the L subunit and some buried water molecules, with M- and H-subunit residues also close by. The effects of site-directed mutagenesis upon RC turnover and quinone function have implicated several L-subunit residues in proton delivery to Q_B, although some species differences exist. In wild-type *Rb. sphaeroides*, Glu^{L212} and Asp^{L213} represent an inner shell of residues of particular importance in proton transfer to Q_B. Asp^{L213} is crucial for delivery of the first proton, coupled to transfer of the second electron, while Glu^{L212}, possibly together with Asp^{L213}, is necessary for delivery of the second proton, after the second electron transfer. We report here the first study, by site-directed mutagenesis, of the role of the H subunit in Q_B function. Glu^{H173}, one of a cluster of strongly interacting residues near Q_B, including Asp^{L213}, was altered to Gln. In isolated mutant RCs, the kinetics of the first electron transfer, leading to formation of the semiquinone, Q_B^-, and the proton-linked second electron transfer, leading to the formation of fully reduced quinol, were both greatly retarded, as observed previously in the $Asp^{L213} \rightarrow$ Asn mutant. However, the first electron transfer equilibrium, $Q_A^-Q_B \rightleftharpoons Q_AQ_B^-$, was decreased, which is opposite to the effect of the $Asp^{L213} \rightarrow$ Asn mutation. These major disruptions of events coupled to proton delivery to Q_B were largely reversed by the addition of azide (N_3^-). The results support a major role for electrostatic interactions between charged groups in determining the protonation state of certain entities, thereby controlling the rate of the second electron transfer. It is suggested that the essential electrostatic effect may be to "potentiate" proton transfer activity by raising the pK of functional entities that actually transfer protons in a coupled fashion with the second electron transfer. Candidates include buried water (H_3O^+) and Ser^{L223} (serine-OH_2^+), which is very close to the O5 carbonyl of the quinone.**

The photosynthetic reaction center (RC) of the purple bacterium, *Rhodobacter (Rb.) sphaeroides*, is an integral membrane protein–pigment complex composed of three subunits (L, M, and H), four bacteriochlorophylls, two bacteriopheophytins, two ubiquinones, and an iron atom. Activation of the RC by a flash results in intraprotein charge separation by electron transfer from the primary donor (P), a dimer of bacteriochlorophyll, to the primary and secondary quinones (Q_A and Q_B, respectively). Cytochrome c_2 reduces P^+, *in vivo*. This first electron is shared by the anionic semiquinones, Q_A^- and Q_B^-, and the negative charge induces pK shifts of nearby ionizable amino acid residues, resulting in protonation of the RC, partial shielding of the charge, and stabilization of Q_B^- (1–3). Second flash activation results in the double reduction of Q_B, coupled with the delivery of two protons, to form a quinol molecule (Q_BH_2), which leaves the RC and is replaced by an oxidized quinone from the membrane pool. This returns the quinones to their original state and allows RC turnover to proceed under multiple-flash activations. Under such conditions, binary oscillations can be seen in the formation and disappearance of semiquinone and in the uptake of protons from the medium (for review, see refs. 4 and 5).

Studies on RCs altered by site-directed mutagenesis strongly implicate two ionizable residues in functional proton transfer to the Q_B binding site in *Rb. sphaeroides*—Glu and Asp at positions 212 and 213, respectively, of the L subunit (6–9). These are the two ionizable residues nearest to the Q_B head group (Fig. 1). Alteration of Asp^{L213} to Asn had severe effects, including a very large increase in the $Q_A^-Q_B \rightleftharpoons Q_AQ_B^-$ equilibrium in favor of Q_B reduction and modification of the pH dependence of the equilibrium, especially at acid pH (7–9). Also, transfer of the second electron to Q_B was almost completely blocked, due to failure in the transfer of the first proton necessary for the double reduction of Q_B:

$$Q_A^-Q_B^- + H^+ —\times\rightarrow Q_AQ_BH^-.$$

Alteration of Glu^{L212} to Gln also had significant effects on the quinone reactions (6, 8). The pH dependences of the $Q_A^-Q_B \rightleftharpoons Q_AQ_B^-$ equilibrium and electron transfer rate at alkaline pH were essentially eliminated, and the rate of transfer of the second proton in the formation of quinol was greatly reduced:

$$Q_BH^- + H^+ —\times\rightarrow Q_BH_2.$$

Although the proximity of Glu^{L212} and Asp^{L213} to Q_B in the *Rb. sphaeroides* RC structure is suggestive of their functional importance, they do not represent a unique solution to the problem of transferring protons to the Q_B site. In the otherwise closely homologous RCs from *Rhodopseudomonas (Rps.) viridis* (10) and *Rhodospirillum (R.) rubrum* (11), as well as the less closely related species *Chloroflexus (Chf.) aurantiacus* (12), the native residue at position L213 is already Asn. However, there is a compensating change at a nearby residue (M43 or M44 in different species), from Asn in *Rb. sphaeroides* to Asp in *Rps. viridis*, *R. rubrum* and *Chf. aurantiacus*, suggesting the general importance of negative charge interactions in the proton transfer function of this domain (13–16). This is strongly

The publication costs of this article were defrayed in part by page charge payment. This article must therefore be hereby marked "*advertisement*" in accordance with 18 U.S.C. §1734 solely to indicate this fact.

Abbreviations: RC, reaction center; P, primary electron donor; Q_A and Q_B, primary and secondary quinone electron acceptors; Wt, wild type.

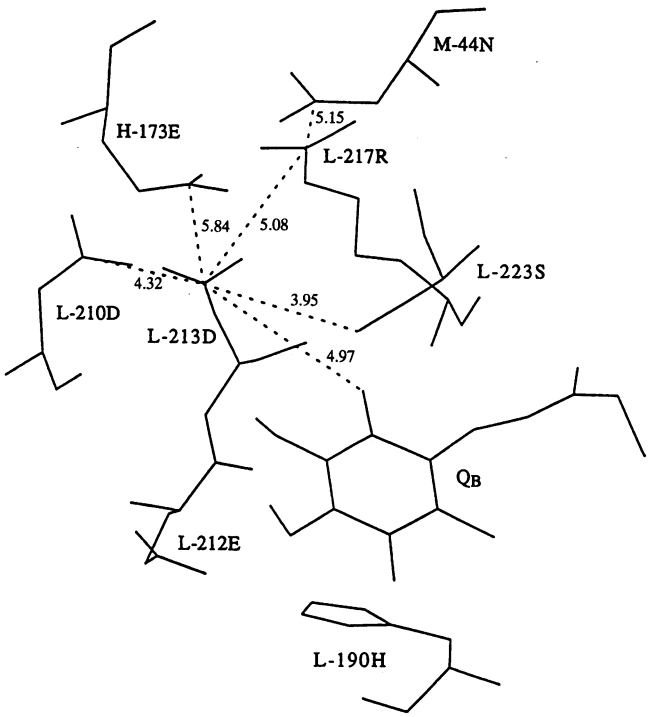

FIG. 1. Q_B binding site of the reaction center from *Rb. sphaeroides* showing various ionizable residues and residues implicated in protonation reactions. The side chain of Q_B has been truncated after the first isoprene unit. Hydrogen bonds are shown by dotted lines. Long-dashed lines connect several selected residues, with the distances given in angstroms.

supported by studies on second-site revertants of an L212/L213 double mutant of *Rhodobacter capsulatus*, in which functionality was restored by the introduction of an acidic (i.e., negatively charged) group at several positions in the general vicinity of the Q_B site, including M43, and one that could be best understood as the removal of a positive charge at a quite distant location (14, 15).

The lack of a clear implication of any one ionizable residue, and the evident significance of general electrostatic influences, has led to the recognition that internal water molecules are equally good candidates for proton carrying functions (14, 17), and modeling studies by Beroza *et al.* (16) showed the potential for internal water molecules to make functionally suggestive connections between residues in the *Rb. sphaeroides* RC.

In vivo, protons involved in the reduction of Q_B come exclusively from the cytosolic side of the membrane. From known RC structures (18–20), the H subunit lies over the cytosolic side of the complex, covering the two quinone-binding sites in the L–M heterodimer. Therefore, polar and ionizable residues of the H subunit, as well as water molecules present therein, may provide pathways for proton delivery to the Q_B binding pocket.

The overall functional significance of the H subunit was explored by Debus *et al.* (21) by removing the H subunit from the RC complex. Although the primary functions of the L–M heterodimer were largely unaffected, major disturbances were observed in the functional characteristics of the two quinones. However, the role of individual residues of the H subunit has not been addressed until now. We report here the first use of site-directed mutation of the H subunit for the study of RC function. We targeted Glu^{H173} because it is near the Q_B binding site (Fig. 1) and, with Asp^{L213}, Asp^{L210}, Arg^{L217}, and Ser^{L223}, forms a cluster of ionizable amino acid side chains with strong electrostatic interactions (5, 13).

MATERIALS AND METHODS

The H-subunit gene (*puhA*) was generously provided by S. Kaplan, as a 8-kb *Eco*RI restriction fragment. The $Glu^{H173} \rightarrow$ Gln mutation was obtained by *in vitro* mutagenesis, as described (8), using an oligonucleotide with an altered codon for amino acid residue 173 (GAG → CAG) of the H-subunit gene. The desired mutation was screened by DNA sequencing. The mutant gene was transferred into the *Rb. sphaeroides* H-subunit deletion strain 601-10 (kanamycin resistant), a derivative of the 2.4.1 wild type (Wt) (22), using the suicide vector pSUP202 and conjugational mating with *Escherichia coli* S17-1 (23). Double recombinants, for expression of mutant RCs in cis, were identified by screening for kanamycin sensitivity.

Cells bearing the $Glu^{H173} \rightarrow$Gln mutation (mutant H173EQ) were initially grown under semiaerobic conditions in the dark, in minimal medium supplemented with yeast extract (5 g/liter), tryptone (3 g/liter) and Casamino acids (1 g/liter), with final anaerobic growth, prior to harvesting, under phototrophic conditions (8). To confirm lack of reversion, chromosomal DNA from harvested cells was isolated and the *puhA* region was amplified by asymmetric polymerase chain reaction and sequenced.

Rb. sphaeroides cells were disrupted by French press, and chromatophores were prepared as described (2). RCs were solubilized by the method of Jolchine and Reiss-Husson (24), in 0.55% lauryl dimethylamine-*N*-oxide and purified by ammonium sulfate precipitation and ion-exchange chromatography on DEAE-Sephacel.

Mutant RCs were characterized by optical spectroscopy performed on a kinetic spectrophotometer apparatus of local design. The assay solution was 2.5 mM KCl/0.017% Triton X-100/33.3 μM ubiquinone (Q-10)/1 mM buffer {succinate, citrate, Mes, Pipes, Tris, Ches [(cyclohexylamino)ethanesulfonic acid], or Caps [3-(cyclohexylamino)-1-propanesulfonic acid], depending on the pH} and ≈1 μM RC. Kinetic assays were carried out as described (8). The kinetics of P^+ dark decay after a flash ($P^+Q_AQ_B^-$ charge recombination) were measured at 430 nm, in the absence of an electron donor to P^+. The kinetics of the first electron transfer from Q_A^- to Q_B were measured at 397 nm, where the spectrum for Q_A^- includes a significant electrochromic response of the nearby bacteriopheophytin. The semiquinone signals of Q_A^- and Q_B^- and the kinetics of the second electron transfer were monitored at 450 nm with 1–200 μM ferrocene as donor to P^+. Cytochrome oxidation was monitored at 550 nm, with 20 μM horse heart cytochrome *c*. All measurements were made at 23°C.

RESULTS

$P^+Q_AQ_B^-$ Charge Recombination: pH Dependence of the One-Electron Transfer Equilibrium. Flash induced electron transfer, within the RC complex, results in the formation of oxidized primary electron donor (P^+) and reduced quinone electron acceptors. With no electron donor to P^+, the P^+ absorbance at 430 nm decays over time due to charge recombination. In the absence of functional Q_B, the relatively fast charge recombination of the $P^+Q_A^-$ state is seen ($k_{AP} \approx 10\,s^{-1}$). k_{AP} is only weakly pH dependent over a wide pH range. Addition of ubiquinone reconstitutes the Q_B lost during the RC isolation procedure, and the observed decay of the P^+ signal is predominantly slow, indicating charge recombination from the more stable $P^+Q_AQ_B^-$ state (Fig. 2*A*). The observed slow back reaction rate, k_{obs}, provides a measure of the equilibrium constant K_{AB} for the one-electron equilibrium between Q_A and Q_B (1, 5, 25, 26):

$$PQ_AQ_B \xleftarrow{k_{AP}} P^+Q_A^-Q_B \rightleftharpoons P^+Q_AQ_B^-, \quad K_{AB}$$

where $K_{AB} = (k_{AP}/k_{obs}) - 1$. This assay is especially good for large values of K_{AB}, i.e., when the signal decay is slow and $k_{obs} \ll k_{AP}$.

The pH dependences of K_{AB} determined from k_{obs} for Wt and H173EQ mutant RCs are shown in Fig. 2*C*. Wt RCs exhibited two pH-dependent regions–below pH ≈5.5 and above pH ≈8.5—separated by a wide plateau. In H173EQ mutant RCs, the slow phase was substantially faster, and the equilibrium constant was correspondingly smaller, than the Wt at all pH values examined, and the two pH-dependent regions were separated by only a narrow plateau at pH 5.5–6.5.

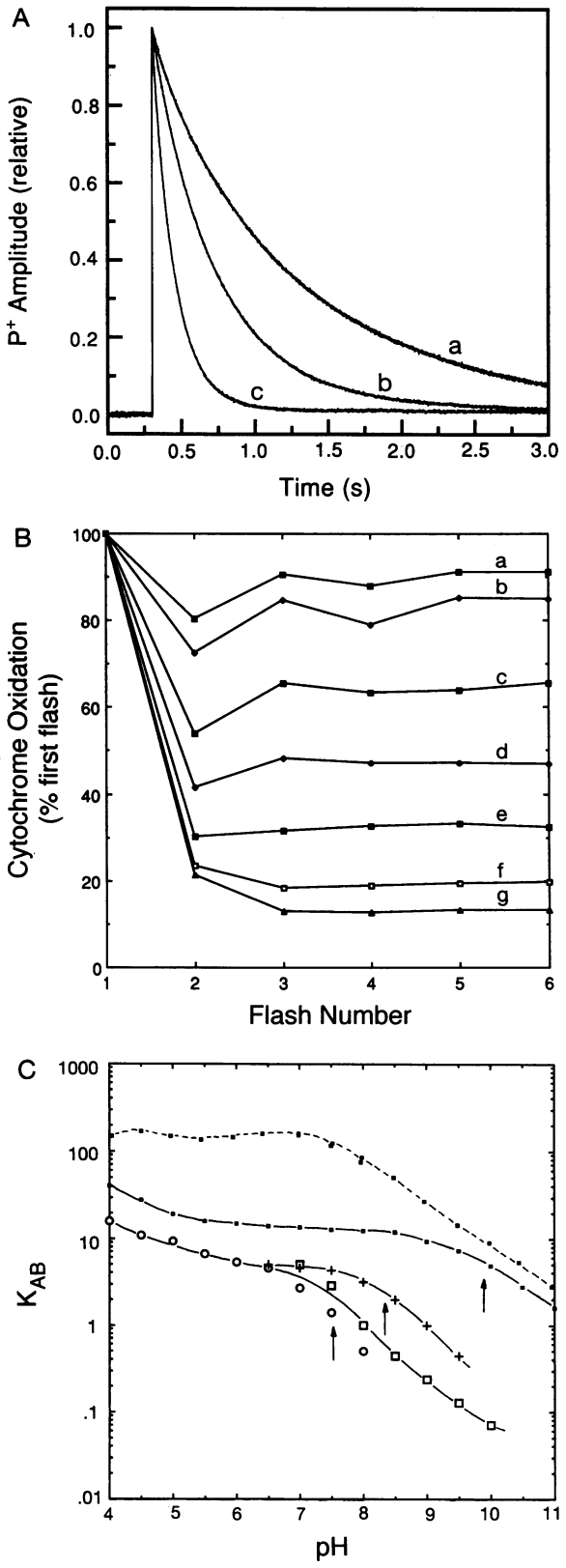

FIG. 2. (*A*) Kinetics of the $P^+Q_AQ_B^-$ charge recombination in Wt and H173EQ mutant RCs, measured at 430 nm. Conditions: 1 μM RC/33 μM Q-10/2.5 mM KCl/0.017% Triton X-100/1 mM buffer, pH 8.0. Traces: a, Wt RCs; b, H173EQ RCs, plus 0.3 M azide; c, H173EQ RCs. (*B*) Cytochrome *c* oxidation by H173EQ mutant RCs in multiple flashes at various pH, measured at 550 nm. For each measurement at a fixed pH, the amount of cytochrome *c* oxidized on the second and subsequent flashes is expressed as a percentage of the amount oxidized on the first flash. Conditions: as for *A*, with 20 μM horse heart cytochrome *c*. Traces: a, pH 7.0; b, pH 7.5; c, pH 8.0; d, pH 8.5; e, pH 9.0; f, pH 9.5; g, pH 10.0. Time between flashes was 0.2 s. (*C*) The pH dependence of the one-electron equilibrium constant K_{AB} for the reaction: $Q_A^-Q_B \rightleftharpoons Q_AQ_B^-$, for H173EQ mutant RCs, determined from the rate of the $P^+Q_AQ_B^-$ charge recombination (○, +) or from the steady cytochrome *c* oxidation (□), with (+) and without (○, □) 0.3 M azide. Data for Wt (points with solid line) and L213DN mutant (points with dashed line) RCs are shown for comparison (from ref. 8). Lines drawn for Wt and H173EQ RCs are fitted in the high pH region with the following pK values: Wt, 9.8 and 11.3; H173EQ, 7.4 and 9.6; H173EQ plus azide, 8.3 and 10.8. The first pK in each case is indicated by an arrow.

The rate of the slow phase in H173EQ RCs increased steadily with pH and the amplitude of the slow phase declined rapidly above pH 7.5 (data not shown), indicating weaker Q_B binding at higher pH. Above pH 8, the slow phase could not be adequately resolved from $P^+Q_A^-$ recombination, but at pH 8, the H173EQ slow-phase recombination rate was more than 10 times faster than the Wt.

RC Turnover in Multiple Flashes: Cytochrome Oxidation. The ability of isolated RCs to perform multiple turnovers, with adequate electron donation to P^+, is a measure of the functional integrity of the quinone electron acceptor activities. Turnover of Wt and H173EQ RCs was monitored at 550 nm via the oxidation of cytochrome *c* in a series of saturating flashes. Progressive inhibition of turnover was seen in the H173EQ RCs above pH 7.0 (Fig. 2*B*), reflecting the accumulation of electrons on Q_A^-. This is due to the increasingly unfavorable equilibrium for transfer of the first electron to Q_B and not to a kinetic limitation in the interquinone electron transfer steps, which are much faster than the flash repetition rate (see below). From the steady-state (*ss*) cytochrome *c* (Cyt *c*) oxidation relative to that on the first flash (*S*), the one-electron equilibrium constant K_{AB}* can be calculated:

$$K_{AB} = \frac{S}{2(1-S)}. \qquad S = \frac{\text{Cyt } c\ (ss)}{\text{Cyt } c\ (1)}.$$

This cytochrome turnover assay is most reliable when K_{AB} is small (e.g., at high pH) and nicely complements the estimate available from the P^+ back reaction data. The pH dependences of K_{AB}, determined by the two methods, overlap quite well (Fig. 2*C*) and indicate a pK of 7.4 associated with the $Q_A^-Q_B$ state, compared to a Wt value of 9.8. A rough value for the pK

*This expression is derived with the following assumptions: (*i*) one electron is shared between $Q_A^-Q_B \rightleftharpoons Q_AQ_B^-$ according to the equilibrium constant K_{AB}, (*ii*) electron pairs are fully transferred out of the acceptor quinone complex, i.e., $Q_A^-Q_B^- \rightarrow Q_AQ_B$ (valid when quinone is present in excess, as used here), and (*iii*) all RCs have functional Q_B activity. The validity of the last assumption is aided by the flash repetition rate used, which allows time for slow turnover of the Q_B site, and is clearly supported by the reasonable agreement between the K_{AB} values calculated from the two methods. A few percent of Q_B-dysfunctional RCs, as normally encountered, would not qualitatively alter the results. Many such expressions, derived from similar underlying recursive relations, have been used to describe the function of the two-electron gate behavior of the acceptor quinones (1, 5, 26, 36).

associated with the $Q_AQ_B^-$ state can be estimated at about pH 9.6, compared to a Wt value of 11.3 (2, 3, 8, 26).

Kinetics of the First Electron Transfer. In Wt RCs, the rate of $Q_A^-Q_B \rightarrow Q_AQ_B^-$ electron transfer, $k_{AB}^{(1)}$, is roughly pH-independent up to about pH 9. At higher pH, it becomes pH-dependent, being rate limited by the requirement to reprotonate some entity with a pK of 9.4–10.0, which is thought to be Glu^{L212} or a closely coupled residue. (pK values obtained from the kinetics of the $Q_A^-Q_B \rightarrow Q_AQ_B^-$ electron transfer tend to be lower than those obtained from the quasiequilibrium assay of the $P^+Q_AQ_B^-$ decay kinetics.)

In H173EQ RCs, the pH dependence of $k_{AB}^{(1)}$ is greatly modified. At very low pH, the rate approaches the Wt value, but it decreases steadily above pH 5 (Fig. 3) in a somewhat complicated manner, as previously found for L213DN mutant RCs (7–9). An inflection in the decline at about pH 6.5 probably indicates a functional pK, in rough correspondence with the pK value seen in the equilibrium data (Fig. 2*C*). Although severely inhibited, the rate of electron transfer from Q_A^- to Q_B was adequate to ensure equilibrium on the time scale of the slow ($P^+Q_AQ_B^-$) recombination process, at all pH values examined ($k_{AB}^{(1)} \geq 10k_{AP}$).

Second Electron Transfer and Semiquinone Oscillations. Semiquinone formation and disappearance were monitored at 450 nm with multiple saturating flashes, in the presence of ferrocene as exogenous electron donor to P^+. Typical semiquinone oscillations, as seen for Wt RCs, were observed only in the low pH region (pH $\leq$ 6.0) for the H173EQ mutant RCs. With increasing pH, the semiquinone oscillations became progressively worse, and none was observed above pH 8.0 (data not shown).

The second electron transfer is indicated by the decay of the semiquinone signal, after the second flash. In Wt RCs, this reaction is strongly pH-dependent and is kinetically coupled to proton transfer to Q_B (1, 6, 8). In H173EQ RCs, the rate of the second electron transfer, $k_{AB}^{(2)}$, was substantially inhibited (Fig. 4), but it accelerated at low pH and approached that observed in Wt RCs at pH <4.5. Above pH 8.5, the rate appeared to level off to a minimum of about 12 s^{-1}. At pH 7.5 and below, the rate was fast enough (>25 s^{-1}) to not limit turnover of the RC in multiple flashes, 0.2 s apart.

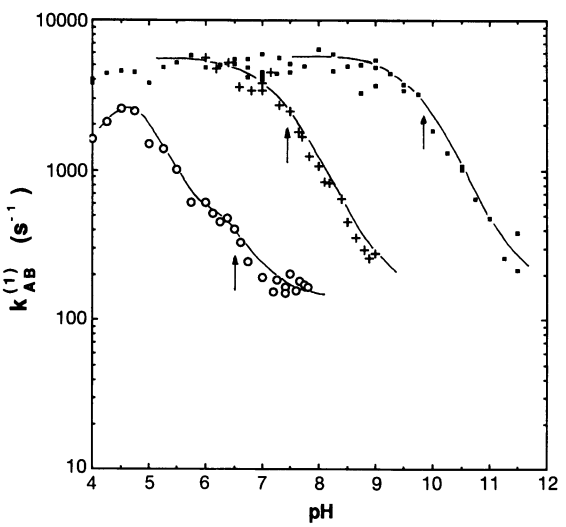

FIG. 3. pH dependence of the rate of the first electron transfer kinetics in Wt and mutant RCs, measured at 397 nm. Conditions for H173EQ mutant RCs as in Fig. 2*A*. Data for Wt RCs are shown for comparison (from ref. 8). Lines drawn for Wt and H173EQ RCs are fitted in the high pH region with the following pK values: Wt (■), 9.7 and 11.3; H173EQ (○), 6.5 and 7.0; H173EQ plus azide (+), 7.4 and 9.0. The first pK in each case is indicated by an arrow.

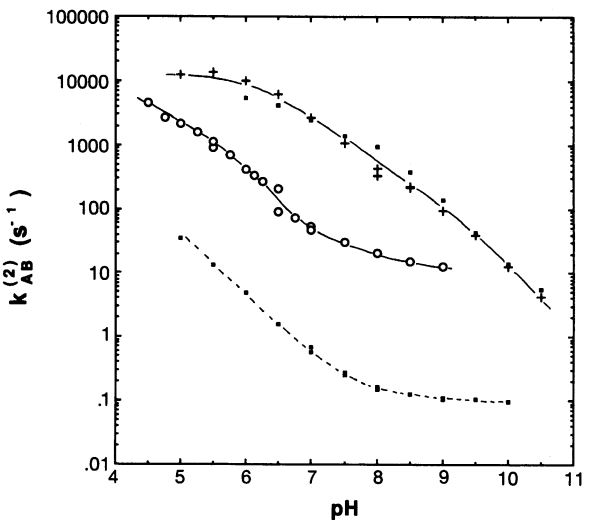

FIG. 4. pH dependence of the rate of the second electron transfer in Wt and mutant RCs, measured at 450 nm. Conditions for H173EQ mutant RCs as in Fig. 2*A*, with ferrocene as donor, added at various concentrations in the range of 1–200 μM to optimize resolution of the semiquinone decay. Data are shown for H173EQ mutant RCs without (○) and with (+) 0.3 M azide. The data for Wt (points with solid line) were redrawn from ref. 1, and for L213DN mutant (points with dashed line) RCs were redrawn from ref. 8.

Effects of Azide on Mutant H173EQ RCs. Azide (N_3^-), a weak acid with pK_a = 4.7, is known to alleviate the impaired second turnover of mutant RCs altered at Glu^{L212} and Asp^{L213} (8, 27). In both cases, it specifically accelerates the mutationally restricted proton transfer to the Q_B pocket. Azide was also formerly shown to "reactivate" certain bacteriorhodopsin mutants and was postulated to act as an intraprotein protonophore (28).

In H173EQ mutant RCs, the addition of 300 mM sodium azide restored the rate of second electron transfer, $k_{AB}^{(2)}$, to Wt rates, over a wide pH range, indicating a substantial effect on the first proton transfer (Fig. 4). This is similar to, but more marked than, its effect on L213DN mutant RCs (8, 27). Addition of 300 mM KCl had no significant effect on these kinetics in either mutant or Wt RCs.

Addition of azide also increased the rate of the first electron transfer $k_{AB}^{(1)}$, accelerating it 20-fold at pH 7 and shifting the apparent pK from 6.5 to about 7.6 (Fig. 3). At low pH (≈6.5), in the presence of azide, $k_{AB}^{(1)}$ closely approached the value in Wt RCs. In control measurements, 300 mM KCl caused the kinetics in H173EQ mutant RCs to become noticeably biphasic, but the average rate was not altered. This interesting effect is under further study.

In addition to its effects on the kinetics of interquinone electron transfer, azide also retarded the slow phase of the back reaction in H173EQ RCs, above pH 6.5 ($P^+Q_AQ_B^-$ recombination) (Fig. 2*C*). The effect on k_{obs} shows azide to increase the one-electron equilibrium constant K_{AB}, and the pK associated with the $Q_A^-Q_B$ state is raised from 7.6 to 8.6. From the shape of the curve, the effect on the pK associated with $Q_AQ_B^-$ is estimated to be similar.

DISCUSSION

The onset of pH dependence for one-electron transfer and equilibrium in Wt RCs at about pH 9 has been attributed to the ionization of Glu^{L212}, with an apparent pK of about 9.5, which is shifted to higher values by electrostatic interaction with Q_B^- (6, 8). Electrostatic calculations on the RC, however, suggested that this residue would be ionized at much lower pH (13), consistent with recent infrared spectroscopic studies (29).

Thus, our understanding of this pH-dependent behavior is unclear and more complex interactions appear to be necessary to account for it. Nevertheless, the dramatic effects of mutation of Asp^{L213} and Glu^{H173} on this functional pK implicate charge–charge interactions as a major influence on the Wt value, rather than, e.g., solvent exclusion.

In the H173EQ RCs, inflections in the pH dependence of first electron transfer functions indicate that the pK in the high pH region has been shifted down from ≈9.5 to ≈7.5 (K_{AB}) or ≈6.5 (k_{AB}) (ΔpK = 2 to 3). A down-shift in the pK also occurred in RCs containing the $Asp^{L213} \rightarrow$ Asn mutation (mutant L213DN) (7, 9). In L213DN RCs, however, the effect was to make the one-electron equilibrium constant very large and the recombination reaction was suggested to proceed directly from Q_B^- to P^+ so that the decay kinetics did not reflect the value of K_{AB} (8). The direct nature of the $P^+Q_B^-$ recombination in this mutant has since been confirmed (30). As discussed (8), therefore, it is possible that the pK shift in the L213DN mutant RCs was from ≈9.5 to as low as 5.0 (ΔpK = 4.5).

The behaviors of both L213DN and H173EQ mutant RCs suggest that the pK in the Wt, as manifested in the stability of Q_B^-, results from electrostatic interactions that include the negative charges of Asp^{L213} and Glu^{H173}, probably as well as Glu^{L212}. The observed pK shifts are consistent with calculations by Gunner and Honig (13) of the energies of interaction between these residues (Table 1).

The effect of the $Glu^{H173} \rightarrow$ Gln mutation on the second electron transfer is striking. The rate, relative to the Wt value, is retarded by a factor of 10^2. This may be compared to the effect of the $Asp^{L213} \rightarrow$ Asn mutation, which slows down the second electron transfer at least 10^4-fold (8, 9). We suggest that these mutants reveal the role of these residues in determining the pK values of certain protonatable entities that are poised to function by electrostatic interactions with the charge cluster. The control of the second electron transfer by pH may arise directly by a rate limiting proton transfer or indirectly by the electrostatic potential or active configuration of the environment, as determined by the equilibrium protonation state of various entities.† In either case, if the rate of the second electron transfer is limited by the protonation state of such an entity, i.e., rate $\alpha\, AH/A_{tot}$, we can estimate the magnitude of the pK shifts induced by the mutations. For simple titration behavior, the fractional, time-averaged degree of protonation is given by:

$$AH/A_{tot} = 1/(1 + 10^{pH\text{-}pK}) \approx 10^{pK\text{-}pH}.$$

(The approximation applies if the prevailing pH is significantly higher than the pK value.) Thus, the effects of removing the negative carboxylates of Glu^{H173} and Asp^{L213} on the kinetics of the second electron transfer translate into decreases in the pK of 2 and 4 units, respectively. We can think, therefore, in terms of a protonatable—and possibly proton-carrying—moiety that is poised to function adequately, near neutral pH, by virtue of these negative charge interactions, and whose pK drops toward its intrinsic and nonfunctional value in their absence.

The electrostatic origin of these mutational lesions is consistent with the effect of azide, as a weakly bound anion, in restoring some degree of functionality. In H173EQ mutant RCs, 300 mM azide completely restored the rate of the second electron transfer, to Wt levels. In L213DN mutant RCs, the restoration was incomplete even at the highest concentration used (863 mM). This may indicate that the binding site for azide is closer to Glu^{H173} than to Asp^{L213}, and the x-ray crystallographic structures of the *Rb. sphaeroides* RC (19, 20, 31) show a substantial cavity in the region of Glu^{H173}, which could provide such a site.

†We do not consider it likely that these substantial decreases in the rate of the second electron transfer could arise from significant structural changes, partly because both first and second electron transfers tend toward Wt rates at low pH, and azide further restores these rates, and partly because the binding affinity for quinone at the Q_B site in these mutants is similar to the Wt rates at pH ≤7.

Table 1. Comparison of calculated and observed magnitudes of interaction between Glu^{L212} and other ionic residues in the Q_B pocket

	Glu^{L212}–Asp^{L213}	Glu^{L212}–Glu^{H173}
ΔpK(obs)*	2.5–4.5†	2–3
ΔG_{int}(obs)*, kcal/mol	3.5–6†	2.5–4
ΔpK(calc)‡	3.8	2.2
ΔG_{int}(calc)‡, kcal/mol	5.2	3.0

*ΔpK is the experimentally observed shift in the functional pK (assigned to Glu^{L212} for simplicity) upon mutation of Asp^{L213} or Glu^{H173} to the neutral amide; ΔG_{int} was obtained from the relationship: $\Delta G_{int} = 2.303RT\cdot\Delta pK$, at $T = 298$ K, and rounded to the nearest half integer.

†Data are from ref. 8.

‡ΔpK is derived, as indicated, from ΔG_{int}, which was calculated in ref. 13.

Candidates for proton-carrying species include internal and bound waters, for which the magnitude of these effects, in terms of electrostatic influences on functional pK values, are especially significant. Many water molecules are revealed in a new higher-resolution (2.3 Å) x-ray structure, including a continuously connected chain that runs from the aqueous interface to the edge of the Q_B pocket (31). With an intrinsic pK for H_3O^+/H_2O close to the solution value of −1.74 (32), the influence of Asp^{L213} would raise the functional pK to above 2, and the effect of Glu^{H173} could be to raise this by another 2 pH units, to pH >4. Interactions with many other residues, as well as desolvation effects, will contribute to the final value, although not all such influences will be in the same direction. Given the intrinsic speed of proton transfer reactions, it is easy to see how such large effects could poise a strong acid to be effective, requiring only a small fraction to be in the protonated form.

Another candidate for a proton carrier is Ser^{L223}, which is close to the O5 carbonyl oxygen of the secondary quinone, and may hydrogen bond to it in the semiquinone state. From textbook values for aliphatic alcohols, we expect the serine hydroxyl to have an intrinsic pK of about −2 (e.g., see ref. 33). Mutant RCs with Ser^{L223} substituted by apolar residues (Ala or Pro) are affected in a similar way to the $Asp^{L213} \rightarrow$ Asn mutant, with severely inhibited second electron transfer function (34, 35).

It is noteworthy that the effects of the H173EQ and L213DN mutants are very similar in some respects but diametrically opposite in others. Thus, both mutants exhibit severe kinetic impairments of proton-limited electron transfer events—on first and second turnovers—but the one-electron equilibrium is greatly increased in the L213DN mutant and decreased in the H173EQ mutant. We explain this by invoking the network of interactions in the charged amino acid cluster including at least Glu^{H173}, Asp^{L213}, Asp^{L210}, and Arg^{L217}. The x-ray structures of the Wt RCs show close proximity (<5 Å) between Glu^{H173}, Asp^{L213}, and Arg^{L217} (Fig. 1), and calculations (13, 37) show both carboxylic acid residues to be partially ionized over a broad pH range. We suggest that mutation of Asp^{L213} to a neutral species removes a (partial) negative charge close to Q_B, thereby stabilizing the Q_B^- anion. Mutation of Glu^{H173}, on the other hand, enhances the ionic interaction between Asp^{L213} and Arg^{L217}, which leads to further ionization of the aspartic carboxylate and increases the negative charge density close to Q_B, thereby destabilizing the Q_B^- anion. In both cases, however, proton transfer is impeded due to disruption of the electro-

static influence of the charge cluster on the functional pKs of the proton pathway.

The effect of azide on the $P^+Q_AQ_B^-$ recombination kinetics (k_{obs}) in H173EQ mutant RCs is especially revealing since this is an assay of the first electron transfer equilibrium and is not limited by rates of proton transfer. This may indicate that azide acts not in a kinetic role, e.g., as a protonophore, but electrostatically, as a bound negative charge—a possibility suggested by Paddock *et al.* (9). The effect on k_{obs} shows azide to increase the one-electron equilibrium constant K_{AB} and raise the pK values associated with the $Q_A^-Q_B$ and $Q_AQ_B^-$ states (Fig. 2*C*), indicating stabilization of the Q_B^- semiquinone anion. While this cannot be accounted for in terms of azide simply adding negative charge to the vicinity (which would be expected to have the opposite effect), it is readily understandable in the context of the proposed interactions among Glu^{H173}, Asp^{L213}, Asp^{L210}, and Arg^{L217}.

We are indebted to S. Kaplan and colleagues (University of Texas Health Science Center, Houston) for advice on *puhA* manipulations and unpublished sequence data. We also thank U. Ermler and H. Michel (Frankfurt) for information from ref. 31, prior to publication. This work was supported by grants from the National Science Foundation (MCB92-08249) and the U.S. Department of Agriculture, Competitive Grants Program (AG92-37306-7692).

1. Wraight, C. A. (1979) *Biochim. Biophys. Acta* **548,** 309–327.
2. Maróti, P. & Wraight, C. A. (1988) *Biochim. Biophys. Acta* **934,** 329–347.
3. McPherson, P. H., Okamura, M. Y. & Feher, G. (1988) *Biochim. Biophys. Acta* **934,** 348–368.
4. Okamura, M. Y. & Feher, G. (1992) *Annu. Rev. Biochem.* **61,** 861–896.
5. Shinkarev, V. P. & Wraight, C. A. (1993) in *The Photosynthetic Reaction Center*, eds. Deisenhofer, J. & Norris, J. R. (Academic, New York), Vol. 1, pp. 193–255.
6. Paddock, M. L., Rongey, S. H., Feher, G. & Okamura, M. Y. (1989) *Proc. Natl. Acad. Sci. USA* **86,** 6602–6606.
7. Takahashi, E. & Wraight, C. A. (1990) *Biochim. Biophys. Acta* **1020,** 107–111.
8. Takahashi, E. & Wraight, C. A. (1992) *Biochemistry* **31,** 855–866.
9. Paddock, M. L., Rongey, S. H., McPherson, P. H., Juth, A., Feher, G. & Okamura, M. Y. (1994) *Biochemistry* **33,** 734–745.
10. Michel, H., Weyer, K. A., Gruenberg, H., Dunger, I., Oesterhelt, D. & Lottspeich, F. (1986) *EMBO J.* **5,** 1149–1158.
11. Bélanger, G., Berard, J., Corriveau, P. & Gingras, G. (1988) *J. Biol. Chem.* **263,** 7632–7638.
12. Ovchinnikov, Y. A., Abdulaev, N. G., Zolotarev, A. S., Shmuckler, B. E., Zargarov, A. A., Kutuzov, M. A., Telezhinskaya, I. N. & Levina, N. B. (1988) *FEBS Lett.* **231,** 237–242.
13. Gunner, M. R. & Honig, B. (1992) in *The Photosynthetic Bacterial Reaction Center II*, eds. Breton, J. & Verméglio, A. (Plenum, New York), pp. 403–410.
14. Hanson, D. K., Baciou, L., Tiede, D. M., Nance, S. L., Schiffer, M. & Sebban, P. (1992) *Biochim. Biophys. Acta* **1102,** 260–265.
15. Hanson, D. K., Tiede, D. M., Nance, S. L., Chang, C.-H. & Schiffer, M. (1993) *Proc. Natl. Acad. Sci. USA* **90,** 8929–8933.
16. Beroza, P., Fredkin, D. R., Okamura, M. Y. & Feher, G. (1992) in *The Photosynthetic Reaction Center II*, eds. Breton, J. & Verméglio, A. (Plenum, New York), pp. 363–374.
17. Maróti, P., Hanson, D. K., Baciou, L., Schiffer, M. & Sebban, P. (1994) *Proc. Natl. Acad. Sci. USA* **91,** 5617–5621.
18. Michel, H., Epp, O. & Deisenhofer, J. (1986) *EMBO J.* **5,** 2445–2451.
19. Allen, J. P., Feher, G., Yeates, T. O., Komiya, H. & Rees, D. C. (1988) *Proc. Natl. Acad. Sci. USA* **85,** 8487–8491.
20. Chang, C.-H., El-Kabbani, O., Tiede, D., Norris, J. R. & Schiffer, M. (1991) *Biochemistry* **30,** 5352–5360.
21. Debus, R. J., Okamura, M. Y. & Feher, G. (1985) *Biochemistry* **24,** 2488–2500.
22. Sockett, R. E., Donohue, T. J., Varga, A. R. & Kaplan, S. (1989) *J. Bacteriol.* **171,** 436–446.
23. Simon, R., Proefer, U. & Puhler, A. (1983) *Bio/Technology* **1,** 784–791.
24. Jolchine, G. & Reiss-Husson, F. (1974) *FEBS Lett.* **40,** 5–8.
25. Mancino, L. J., Dean, D. P. & Blankenship, R. E. (1984) *Biochim. Biophys. Acta* **764,** 46–54.
26. Kleinfeld, D., Okamura, M. Y. & Feher, G. (1984) *Biochim. Biophys. Acta* **766,** 126–140.
27. Takahashi, E. & Wraight, C. A. (1991) *FEBS Lett.* **283,** 140–144.
28. Tittor, J., Soell, C., Oesterhelt, D., Butt, H. J. & Bamberg, E. (1989) *EMBO J.* **8,** 3477–3482.
29. Hienerwadel, R., Grzybek, S., Fogel, C., Kreutz, W., Okamura, M. Y., Paddock, M. L., Breton, J., Nebedryk, E. & Mäntele, W. (1995) *Biochemistry* **34,** 2832–2843.
30. Labahn, A., Paddock, M. L., McPherson, P. H., Okamura, M. Y. & Feher, G. (1994) *J. Phys. Chem.* **98,** 3417–3423.
31. Ermler, U., Fritzsch, G., Buchanan, S. K. & Michel, H. (1995) *Curr. Biol.* **2,** 925–936.
32. Gutman, M. & Nachliel, E. (1990) *Biochim. Biophys. Acta* **1015,** 392–414.
33. Lowry, T. H. & Richardson, K. S. (1981) *Mechanism and Theory in Organic Chemistry* (Harper and Row, New York), 2nd Ed., p. 280.
34. Paddock, M. L., McPherson, P. H., Okamura, M. Y. & Feher, G. (1990) *Proc. Natl. Acad. Sci. USA* **87,** 6803–6807.
35. Paddock, M. L., Rongey, S. H., Abresch, E. C., Okamura, M. Y. & Feher, G. (1988) *Photosynth. Res.* **17,** 75–96.
36. Kleinfeld, D., Abresch, E. C., Okamura, M. Y. & Feher, G. (1984) *Biochim. Biophys. Acta* **765,** 406–409.
37. Beroza, P., Fredkin, D. R., Okamura, M. Y. & Feher, G. (1995) *Biophys. J.* **68,** 2233–2250.